AGU PUBLICATIONS

Geophysical Research Letters

RESEARCH LETTER
10.1002/2017GL075104

Key Points:
- Low-frequency hiss can bounce-resonate efficiently with near-equatorially mirroring electrons
- Bounce resonance has a strong dependence on electron equatorial pitch-angle
- Quantitative differences are presented among the bounce, cyclotron and Landau resonant scattering of electrons.

Correspondence to:
B. Ni,
bbni@whu.edu.cn

Citation:
Cao, X., Ni, B., Summers, D., Zou, Z., Fu, S., & Zhang, W. (2017). Bounce resonance scattering of radiation belt electrons by low-frequency hiss: Comparison with cyclotron and Landau resonances. *Geophysical Research Letters, 44*, 9547–9554. https://doi.org/10.1002/2017GL075104

Received 27 JUL 2017
Accepted 18 SEP 2017
Accepted article online 21 SEP 2017
Published online 5 OCT 2017

Bounce Resonance Scattering of Radiation Belt Electrons by Low-Frequency Hiss: Comparison With Cyclotron and Landau Resonances

Xing Cao[1], Binbin Ni[1], Danny Summers[2], Zhengyang Zou[1], Song Fu[1], and Wenxun Zhang[1]

[1]Department of Space Physics, School of Electronic Information, Wuhan University, Wuhan, China, [2]Department of Mathematics and Statistics, Memorial University of Newfoundland, St. John's, Newfoundland and Labrador, Canada

Abstract Bounce resonant interactions with magnetospheric waves have been proposed as an important contributing mechanism for scattering near-equatorially mirroring electrons by violating the second adiabatic invariant associated with the electron bounce motion along a geomagnetic field line. This study demonstrates that low-frequency plasmaspheric hiss with significant wave power below 100 Hz can bounce resonate efficiently with radiation belt electrons. By performing quantitative calculations of pitch angle scattering rates, we show that low-frequency hiss-induced bounce resonant scattering of electrons has a strong dependence on equatorial pitch angle α_{eq}. For electrons with α_{eq} close to 90°, the timescale associated with bounce resonance scattering can be comparable to or even less than 1 h. Cyclotron and Landau resonant interactions between low-frequency hiss and electrons are also investigated for comparisons. It is found that while the bounce and Landau resonances are responsible for the diffusive transport of near-equatorially mirroring electrons to lower α_{eq}, pitch angle scattering by cyclotron resonance could take over to further diffuse electrons into the atmosphere. Bounce resonance provides a more efficient pitch angle scattering mechanism of relativistic (≥1 MeV) electrons than Landau resonance due to the stronger scattering rates and broader resonance coverage of α_{eq}, thereby demonstrating that bounce resonance scattering by low-frequency hiss can contribute importantly to the evolution of the electron pitch angle distribution and the loss of radiation belt electrons.

1. Introduction

As an incoherent and broadband whistler mode emission, plasmaspheric hiss is preferentially observed inside the plasmasphere or a detached plasma plume (Meredith et al., 2004; Summers et al., 2008; Thorne et al., 1973). The cyclotron resonant interactions between plasmaspheric hiss and electrons have been shown to account for the formation of the slot region between the inner and outer radiation belts and the decay of energetic and relativistic outer zone electrons (Meredith et al., 2007; Ni et al., 2013; Summers et al., 2007a). Previous observations (Meredith et al., 2007, 2009) have suggested that wave frequencies of plasmaspheric hiss are typically confined between ~100 and several kilohertz. However, a recent study of Li et al. (2013) reported an unusual intensification of plasmaspheric hiss emissions observed by the Van Allen Probes (Mauk et al., 2013) which occurred at wave frequencies down to ~20 Hz and with a peak frequency ~40 Hz, well below the typical hiss wave frequencies. Subsequent statistical studies suggested that plasmaspheric hiss with frequencies below 100 Hz can be observed frequently in the dayside magnetosphere during geomagnetically active conditions (Li et al., 2015) and the corresponding averaged intensities could be even stronger than that for typical hiss emissions (Spasojevic et al., 2015; Tsurutani et al., 2015).

It has been proposed by Shprits (2009) that magnetosonic and H^+ band electromagnetic ion cyclotron (EMIC) waves, which have frequencies comparable to the electron bounce frequency or its harmonics, have the potential to bounce resonate with near-equatorially mirroring electrons by violating the second invariant associated with the electron bounce motion. Bounce resonant interactions with magnetosonic and H^+ band EMIC waves have been subsequently proved by recent studies (e.g., Chen et al., 2015; Cao et al., 2017; Li et al., 2015; Shprits, 2016; Tao & Li, 2016; Tao et al., 2016) to account for the pitch angle scattering of electrons with ~90° equatorial pitch angles. For typical plasmaspheric hiss with wave frequencies much higher than the electron bounce frequency, its bounce resonance with near-equatorially mirroring electrons tends to be insignificant. However, unusually low-frequency hiss with wave frequencies a few to tens of times

the electron bounce frequency can interact potentially with radiation belt electrons by means of bounce resonance (Roberts & Schulz, 1968), which however receives little attention.

While cyclotron resonant interactions between plasmaspheric hiss and electrons have been comprehensively analyzed, it still remains to investigate how bounce resonance with low-frequency hiss influences the radiation belt electron dynamics. In order to understand the electron scattering effects of low-frequency hiss, we perform calculations of bounce resonant pitch angle diffusion coefficients. We demonstrate that low-frequency hiss with significant wave power below 100 Hz can provide an efficient mechanism for scattering near-equatorially electrons to lower equatorial pitch angles.

2. Observations of Low-Frequency Hiss

We focus on a previously reported low-frequency hiss event on 30 September 2012 observed by the Electric and Magnetic Field Instrument Suite and Integrated Science (EMFISIS) instrument (Kletzing et al., 2013) on board the Van Allen Probe A. Figure 1a shows the ambient plasma density inferred from the upper hybrid resonance frequency f_{UHR} identified by the high-frequency receiver channel of EMFISIS. Figures 1b–1f illustrate the frequency-time spectrogram of the electric field spectral density, magnetic field spectral density, wave normal angle, and ellipticity of this broadband electromagnetic wave. During the time interval of wave occurrence, the plasma density increases from ~200 cm^{-3} to ~1000 cm^{-3}, suggesting the presence of this wave event inside the plasmasphere. The majority of the wave power is found below the local lower hybrid resonance frequency f_{LHR} which is shown as a black line in Figures 1b and 1c. Figures 1d and 1e show that these waves are quasi-parallel propagating and right-hand elliptically polarized, indicating that the waves are plasmaspheric hiss rather than magnetosonic waves (Thorne, 2010). This low-frequency hiss emission was identified at frequencies $\gtrsim$30 Hz to ~1000 Hz from the beginning of the event, and the emission subsequently intensified at frequencies ~20 to 100 Hz from L = ~5.2 down to $L < 4$. A further investigation of wave spectral intensities was performed to understand the frequency spectral features of the low-frequency hiss. The power spectral intensities at L = 5.0 ± 0.1, 4.5 ± 0.1 and 4.0 ± 0.1 during the intensification of the low-frequency hiss are shown as line plots in Figures 1f–1h, respectively. The thick black line denotes the mean profile of the hiss spectral intensities. It is shown that the wave power peaks at ~40 Hz, well below the lower cutoff frequency (~100 Hz) of typical hiss. The mean spectral intensity at L = 5 is stronger than at L = 4 and 4.5. The majority of the wave power is confined to the frequency range, 20–150 Hz; the corresponding average wave amplitudes are 146 pT, 135 pT, and 187 pT at L = 4, 4.5, and 5, respectively.

3. Numerical Results

The resonance condition for bounce resonant wave-particle interactions can be written as follows (e.g., Cao et al., 2017; Roberts & Schulz, 1968; Shprits, 2009, 2016):

$$f = l f_b, \tag{1}$$

where f is the wave frequency (in Hz), l is the bounce resonance order, $f_b = \beta c/(4LR_E T(\alpha_{eq}))$ is the particle bounce frequency, $\beta = v/c$, v is the velocity of particle, c is the velocity of light, L is the McIlwain L shell value, R_E is the Earth's radius, and $T(\alpha_{eq}) = 1.3802 - 0.31987\left(\sin(\alpha_{eq}) + \sqrt{\sin(\alpha_{eq})}\right)$.

In Figure 2, we show the bounce resonance order l for hiss of the indicated frequency for α_{eq} = 90° electrons as a function of L shell, corresponding to three specific electron energies E_k = 0.2, 1, and 5 MeV. The black, blue, and red lines correspond to the wave frequencies f = 20, 100, and 150 Hz, respectively. We see that the resonance order increases with L shell and decreases with electron energy. The resonance order can be as low as ~5 for f = 20 Hz and increases significantly with increasing wave frequency. For wave frequencies >100 Hz, the corresponding resonance orders are mostly larger than 20.

To investigate quantitatively the bounce resonant interactions between low-frequency hiss and radiation belt electrons, we calculate the corresponding bounce resonance scattering rates following the method of Tao and Li (2016). The scattering rates are the summation over the bounce resonance order l from the lowest to the highest order and are proportional to the wave power spectral intensity. Figure 2 shows that as the wave frequency increases, the bounce resonance order l increases significantly. Since the majority of the wave power is found at frequencies below 150 Hz as shown in Figure 1, only the contributions from $l \leq 50$ to the electron pitch angle scattering are included in our calculations. The high resonance orders above 50

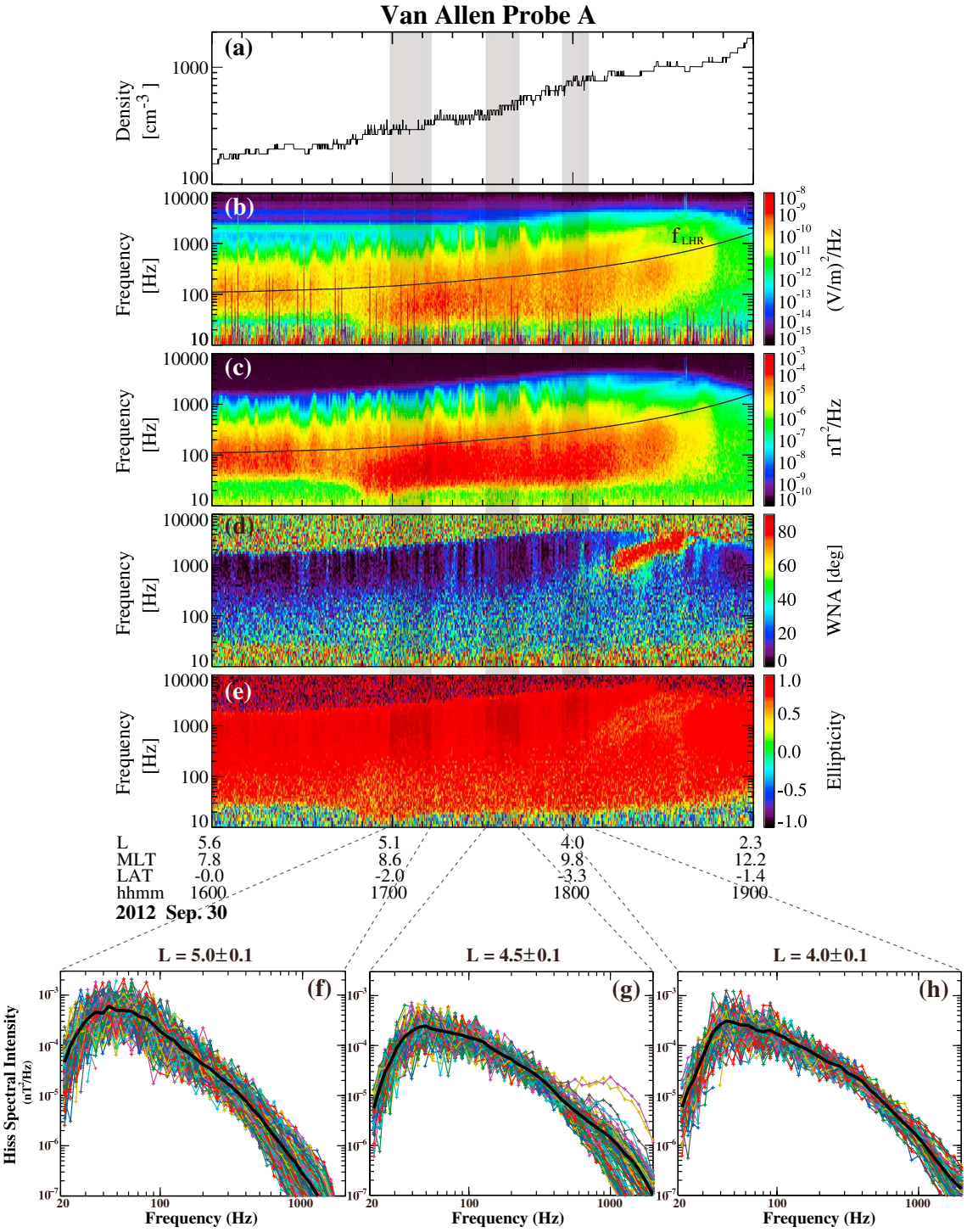

Figure 1. (a) Ambient plasma density inferred from the upper hybrid frequency f_{UHR}. (b and c) Frequency-time spectrogram of electric and magnetic field spectral density, (d) wave normal angle, and (f) ellipticity measured by EMFISIS on board the Van Allen probe A. (f–h) Lines plots of the wave spectral intensities of low-frequency hiss at L = 5.0±0.1, 4.5±0.1, and 4.0±0.1. In Figures 1b and 1c, the black line represents the lower hybrid frequency f_{LHR}. In Figures 1f–1h, the thick black line represents the mean profile of the low-frequency hiss spectral intensity.

can also contribute to the bounce resonant scattering; however, their effects can be negligible due to the much weaker spectral intensity at the corresponding wave frequency and the much reduced occurrence possibility. Using the mean spectral intensities of the hiss waves in Figures 1f–1h (without any Gaussian fit), we perform the calculations at three spatial locations (L = 4, 4.5, and 5) for this intense low-frequency hiss

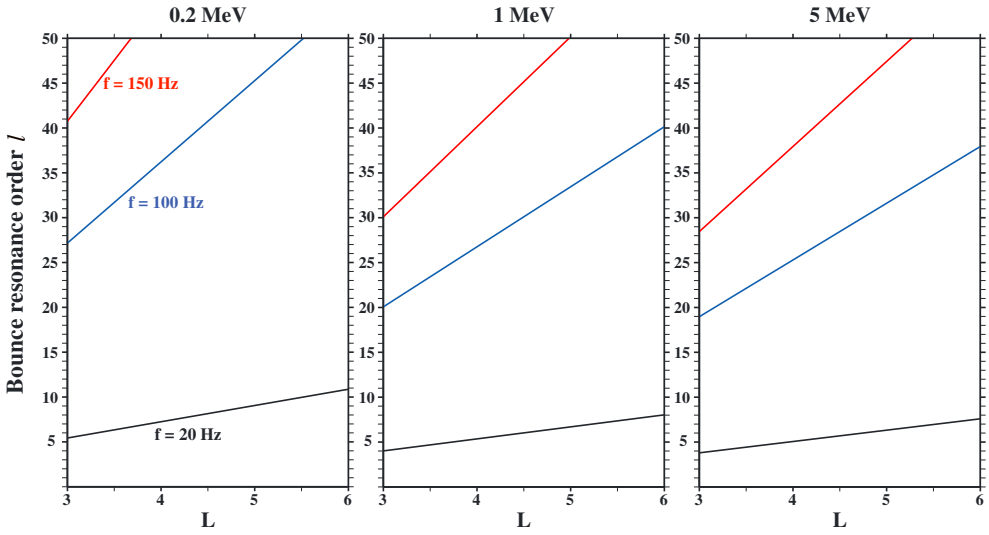

Figure 2. Bounce resonance order as a function of L shell for resonant interactions between radiation belt electrons and low-frequency hiss corresponding to three specific electron kinetic energies E_k (0.2, 1, and 5 MeV) and three specific wave frequencies f (20, 100, and 150 Hz).

event. The geomagnetic field is assumed to be dipolar, and the plasma density shown in Figure 1a is inferred from the upper hybrid resonance frequency. Following the study of Ni et al. (2014), we assume that the maximum latitudinal coverage of this low-frequency hiss event is 30°. Based on the Van Allen Probe A measurements of wave normal angle as shown in Figure 1d, we assume that the hiss wave normal angle θ distribution follows a Gaussian function of $\exp\left[-\left(\frac{\tan\theta-\tan\theta_m}{\tan\theta_w}\right)^2\right]$, where the peak wave normal angle θ_m is assumed to be 20° and the angular width θ_w is assumed to be 30°. The lower and upper boundaries of the wave normal angle distribution are taken to be 0° and 45°, respectively.

In Figure 3 we plot the electron pitch angle scattering rates $D_{\alpha\alpha}$ due to bounce resonant interactions with low-frequency hiss as a function of electron kinetic energy E_k and equatorial pitch angle α_{eq} at L = 4, 4.5, and 5. It is shown that low-frequency hiss could bounce resonate efficiently with near-equatorially mirroring electrons at energies ranging from 10 keV to 10 MeV. The scattering efficiency at L = 5 is found to be much stronger than that at L = 4 and 4.5, which is mainly due to the stronger hiss wave spectral intensities (as shown in Figure 1) and lower geomagnetic field intensity at L = 5 (Cao et al., 2017; Tao & Li, 2016). Figure 3 illustrates that the bounce resonant pitch angle scattering rates have a pronounced dependence on the electron equatorial pitch angle α_{eq}. The scattering efficiency of electrons increases significantly as α_{eq} increases. Especially for electrons with α_{eq} very close to 90°, the timescale associated with pitch angle scattering could be even less than 1 h. It is also found that >100 keV electrons are pitch angle scattered more effectively by low-frequency hiss than lower energy electrons. The higher resonance order that reduces the bounce resonant scattering efficiency at low electron energies (e.g., Shprits, 2016), and the much weaker intensity at the corresponding resonant frequency should be responsible for the weaker pitch angle scattering of <100 keV electrons.

To make quantitative comparisons among the bounce resonance, cyclotron resonance and Landau resonance-induced pitch angle scattering of electrons, the Full Diffusion Code (Cao et al., 2016; Ni et al., 2008, 2015; Shprits & Ni, 2009) is used to calculate the quasi-linear bounce-averaged pitch angle scattering rates due to cyclotron and Landau resonances with low-frequency hiss. The resonance condition for cyclotron and Landau resonant interactions between electrons and electromagnetic waves is given by (Summers et al., 2007b; Summers & Thorne, 2003)

$$\omega - k_{||} v_{||} = N|\Omega_e|/\gamma, \tag{2}$$

where $\omega = 2\pi f$ is the wave frequency, $k_{||}$ is the parallel component of wave number, $v_{||}$ is the electron parallel velocity, Ω_e is the nonrelativistic electron gyro-frequency, $\gamma = (1 - v^2/c^2)^{-1/2}$ is the Lorentz factor, and N is the resonance harmonic. Equation (2) corresponds to the Landau resonance condition when

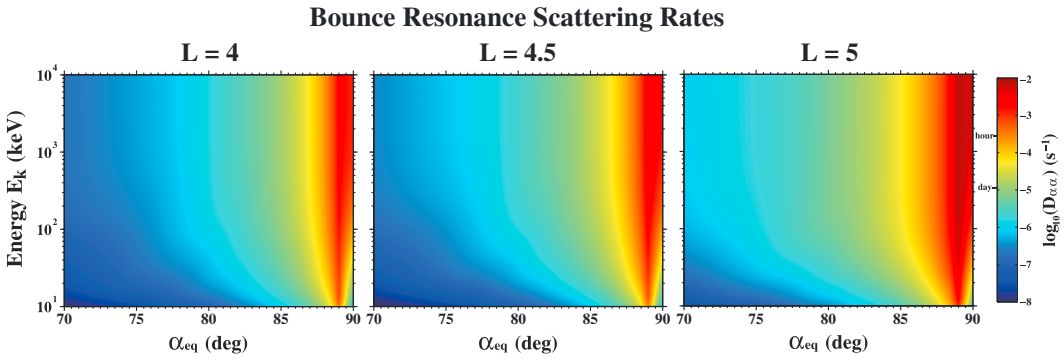

Figure 3. Bounce resonance pitch angle scattering rates by low-frequency hiss as a function of electron energy E_k and equatorial pitch angle α_{eq} at L = 4, 4.5, and 5.

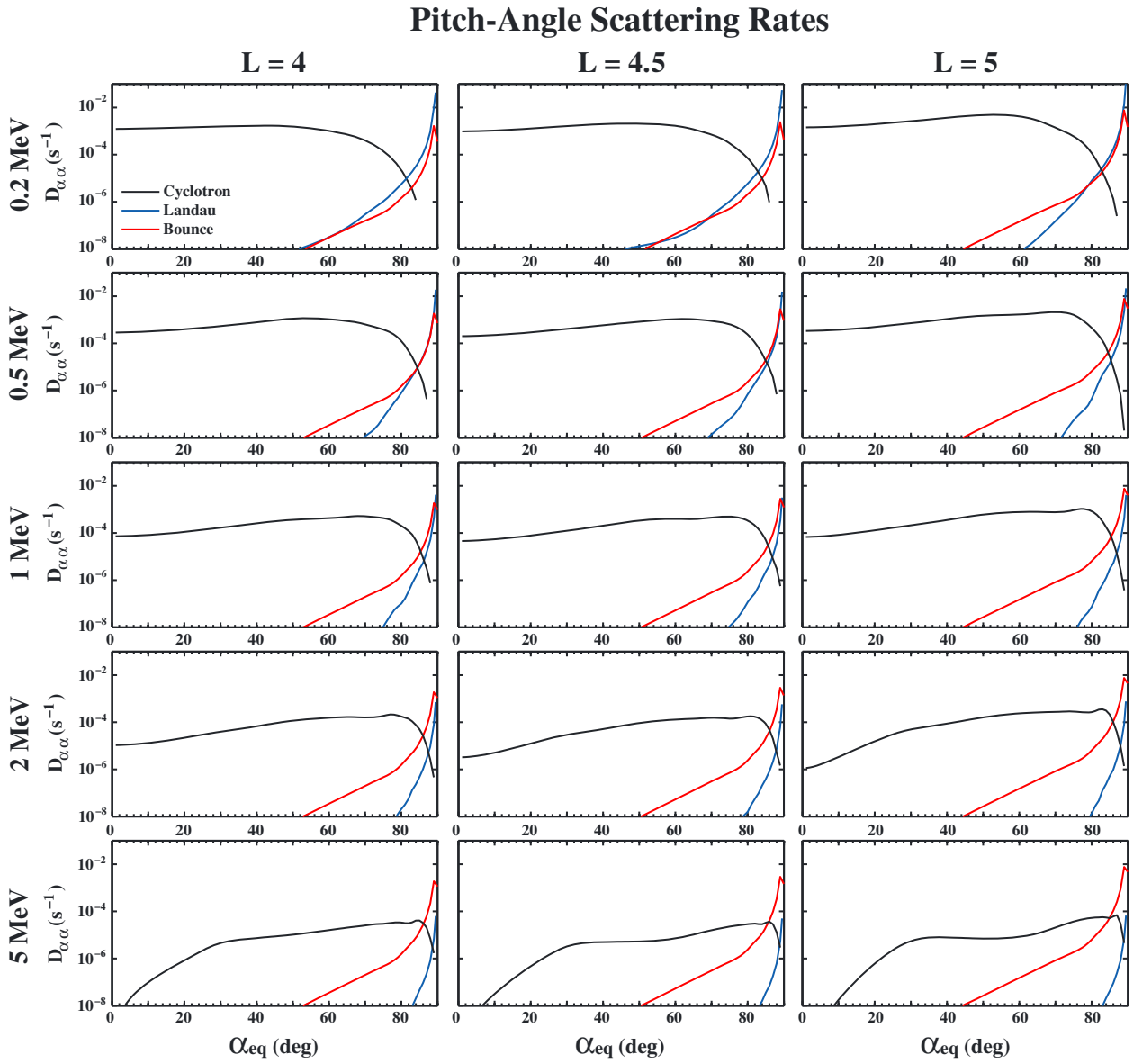

Figure 4. Line plots of low-frequency hiss induced pitch angle scattering rates at L = 4, 4.5, and 5 for five specific electron energies (0.2, 0.5, 1, 2, and 5 MeV). The black, blue, and red lines correspond to the pitch angle scattering due to cyclotron, Landau, and bounce resonances, respectively.

$N = 0$ and corresponds to the cyclotron resonance condition when $N = \pm1, \pm2, \pm3, \ldots$. Electron pitch angle scattering rates due to cyclotron resonance with low-frequency hiss are obtained by including the contributions from cyclotron resonance harmonics $N = -10$ to $N = 10$.

Line plots of low-frequency hiss-induced electron pitch angle scattering rates for five specific electron energies (0.2, 0.5, 1, 2, and 5 MeV) are shown in Figure 4. From left to right, we show the electron pitch angle scattering rates at $L = 4$, 4.5, and 5. The black, blue, and red lines correspond to the scattering rates due to cyclotron, Landau and bounce resonances, respectively. All the parameter values used to calculate the pitch angle scattering rates by cyclotron and Landau resonances are identical to those used to calculate the pitch angle scattering rates by bounce resonance. Figure 4 shows that these three resonance mechanisms occur over two distinct equatorial pitch angle coverages. While bounce and Landau resonance mechanisms are responsible for the pitch angle scattering of near-equatorially mirroring electrons, cyclotron resonant scattering contributes to the diffusive transport of low equatorial pitch angle electrons. While Landau resonance can extend to higher equatorial pitch angles very close to 90° as electron energy increases, there remains an upper limit of equatorial pitch angles above which Landau resonance between low-frequency hiss and radiation belt electrons does not occur. Therefore, we suggest that cyclotron resonance, together with bounce and Landau resonances, could efficiently pitch angle scatter electrons from $\alpha_{eq} \sim 90°$ all the way down to the loss cone and subsequently result in the precipitation loss into the atmosphere.

It is also shown in Figure 4 that pitch angle scattering by Landau resonance is comparable to that by bounce resonance for $\leq$0.5 MeV near-equatorially mirroring electrons. However, due to the significant decrease of Landau-resonant scattering rates with increasing electron energy, bounce resonance can scatter $\geq$1 MeV electrons much more effectively than Landau resonance due to the stronger scattering rates and broader resonance coverage of α_{eq}. This dominance of bounce resonance in scattering $\geq$1 MeV electrons is found to be more pronounced at higher L shells due to the stronger bounce resonant scattering rates. Furthermore, Figure 4 illustrates that cyclotron resonance driven pitch angle scattering of lower α_{eq} electrons is strongly energy dependent. The corresponding scattering efficiency near the loss cone decreases with electron energy and can be negligible when electron energies are larger than 2 MeV.

4. Discussion and Summary

Cyclotron resonant interactions with magnetospheric waves, including plasmaspheric hiss, chorus and EMIC waves, play an essential role in the loss of radiation belt electrons (e.g., Li et al., 2007; Millan & Thorne, 2007; Ni et al., 2015; Shprits et al., 2008; Summers et al., 2007a; Thorne, 2010). However, this cyclotron resonance mechanism cannot resonate with ~90° α_{eq} electrons, suggesting that another potential mechanism affecting electrons mirroring very close to the magnetic equator is required to account for the global coherency of electron fluxes (Shprits, 2009). This study demonstrates that in addition to magnetosonic and H^+ band EMIC waves (e.g., Cao et al., 2017; Shprits, 2016; Tao & Li, 2016), low-frequency hiss with significant wave power below 100 Hz can also bounce resonate with near-equatorially mirroring electrons. While it is assumed that low-frequency hiss is present up to 30° of magnetic latitude, for which the coherency of low-frequency hiss is uncertain, it is worthwhile to point out that our results of bounce resonant electron scattering rates by low-frequency hiss are hardly affected by the broad latitudinal coverage of the waves because the major bounce resonant process only occurs for very high equatorial pitch angle electrons with equatorial low-frequency hiss, as shown in Figures 3 and 4. The confinement of bounce resonant interactions between low-frequency hiss and electrons to the equatorial region also justifies the adoption of a latitudinally constant wave normal angle model for evaluations of bounce resonant scattering rates, while the latitudinal variation of hiss wave normal angle distribution can be important to the wave-induced cyclotron resonant scattering rates (e.g., Ni et al., 2013).

It is also shown in Figure 4 that low-frequency hiss alone cannot cause the loss of ultrarelativistic ($>$ 2 MeV) electrons because there is no cyclotron resonance involving these electrons near the loss cone. We suggest that once EMIC waves are present simultaneously, the rapid scattering loss of low equatorial pitch angle electrons by cyclotron resonance with EMIC waves (Albert, 2003; Summers & Thorne, 2003; Usanova et al., 2014), in combination with the scattering by bounce resonance with low-frequency hiss, can lead to significant losses of the ultrarelativistic electron population. Therefore, bounce resonance scattering by low-frequency hiss should be incorporated into the global modeling of the radiation belt electron

dynamics so as to better understand the evolution of the electron pitch angle distribution, as well as the loss of radiation belt electrons. This, however, is left as a future study.

By evaluating bounce resonant scattering effects of a low-frequency hiss event observed by the Van Allen Probe A, we have shown that bounce resonance can efficiently pitch angle scatter electrons from ~90° α_{eq} to lower α_{eq}. The bounce resonance order decreases with increasing electron energy and decreasing L shell and can be as low as ~5 at the lower cutoff frequency. The scattering efficiency due to bounce resonance is found to be strongly dependent on α_{eq}, and the corresponding timescale could be comparable to or even less than 1 h for electrons with α_{eq} very close to 90°. We have demonstrated that bounce resonance with low-frequency hiss can scatter $>$100 keV electrons more efficiently than $<$100 keV electrons. Quantitative comparisons among cyclotron, Landau and bounce resonances with low-frequency hiss have been performed. Our results suggest that while Landau and bounce resonances are responsible for the diffusive transport of near-equatorially mirroring electrons to lower α_{eq}, cyclotron resonance can take over to subsequently scatter them into the loss cone, leading to the precipitation loss. We find that Landau resonant scattering rates are comparable to bounce resonant scattering rates for $\leq$0.5 MeV electrons. However, due to the significant decrease of the scattering efficiency by Landau resonance as the electron energy increases, it is the bounce resonance that dominates the pitch angle scattering of relativistic ($\geq$1 MeV) electrons that mirror near the geomagnetic equator.

Acknowledgments

The work was supported by the NSFC grants 41674163, 41474141, and 41204120 and the Hubei Province Natural Science Excellent Youth Foundation (2016CFA044). D. S. acknowledges support from a Discovery Grant of the Natural Sciences and Engineering Research Council of Canada. We thank the Van Allen Probes EMFISIS Science Team including Craig Kletzing, William Kurth, and George Hospodarsky for providing the data. The EMFISIS data are obtained from https://emfisis.physics.uiowa.edu/data/index. We would like to thank the reviewers for valuable comments and suggestions. The input files and results of numerical calculations are available from the authors upon request (bbni@whu.edu.cn).

References

Albert, J. M. (2003). Evaluation of quasi-linear diffusion coefficients for EMIC waves in a multispecies plasma. *Journal of Geophysical Research*, *108*(A6), 1249. https://doi.org/10.1029/2002JA009792

Cao, X., Ni, B., Liang, J., Xiang, Z., Wang, Q., Shi, R., … Liu, J. (2016). Resonant scattering of central plasma sheet protons by multiband EMIC waves and resultant proton loss timescales. *Journal of Geophysical Research: Space Physics*, *121*, 1219–1232. https://doi.org/10.1002/2015JA021933

Cao, X., Ni, B., Summers, D., Bortnik, J., Tao, X., Shprits, Y. Y., … Wang, Q. (2017). Bounce resonance scattering of radiation belt electrons by H^+ band EMIC waves. *Journal of Geophysical Research: Space Physics*, *122*, 1702–1713. https://doi.org/10.1002/2016JA023607

Chen, L., Maldonado, A., Bortnik, J., Thorne, R. M., Li, J., Dai, L., & Zhan, X. (2015). Nonlinear bounce resonances between magnetosonic waves and equatorially mirroring electrons. *Journal of Geophysical Research: Space Physics*, *120*, 6514–6527. https://doi.org/10.1002/2015JA021174

Kletzing, C. A., Kurth, W. S., Acuna, M., MacDowall, R. J., Torbert, R. B., Averkamp, T., … Tyler, J. (2013). The Electric and Magnetic Field Instrument Suite and Integrated Science (EMFISIS) on RBSP. *Space Science Reviews*, *179*, 127–181. https://doi.org/10.1007/s11214-013-9993-6

Li, W., Ma, Q., Thorne, R. M., Bortnik, J., Kletzing, C. A., Kurth, W. S., … Nishimura, Y. (2015). Statistical properties of plasmaspheric hiss derived from Van Allen Probes data and their effects on radiation belt electron dynamics. *Journal of Geophysical Research: Space Physics*, *120*, 3393–3405. https://doi.org/10.1002/2015JA021048

Li, W., Shprits, Y. Y., & Thorne, R. M. (2007). Dynamic evolution of energetic outer zone electrons due to wave-particle interactions during storms. *Journal of Geophysical Research*, *112*, A10220. https://doi.org/10.1029/2007JA012368

Li, W., Thorne, R. M., Bortnik, J., Reeves, G. D., Kletzing, C. A., Kurth, W. S., … Thaller, S. A. (2013). An unusual enhancement of low-frequency plasmaspheric hiss in the outer plasmasphere associated with substorm-injected electrons. *Geophysical Research Letters*, *40*, 3798–3803. https://doi.org/10.1002/grl.50787

Li, X., Tao, X., Lu, Q., & Dai, L. (2015). Bounce resonance diffusion coefficients for spatially confined waves. *Geophysical Research Letters*, *42*, 9591–9599. https://doi.org/10.1002/2015GL066324

Mauk, B. H., Fox, N. J., Kanekal, S. G., Kessel, R. L., Sibeck, D. G., & Ukhorskiy, A. (2013). Science objectives and rationale for the radiation belt storm probes mission. *Space Science Reviews*, *179*, 3–27. https://doi.org/10.1007/s11214-012-9908-y

Meredith, N. P., Horne, R. B., Glauert, S. A., & Anderson, R. R. (2007). Slot region electron loss timescales due to plasmaspheric hiss and lightning-generated whistlers. *Journal of Geophysical Research*, *112*, A08214. https://doi.org/10.1029/2007JA012413

Meredith, N. P., Horne, R. B., Glauert, S. A., Baker, D. N., Kanekal, S. G., & Albert, J. M. (2009). Relativistic electron loss timescales in the slot region. *Journal of Geophysical Research*, *114*, A03222. https://doi.org/10.1029/2008JA013889

Meredith, N. P., Horne, R. B., Thorne, R. M., Summers, D., & Anderson, R. R. (2004). Substorm dependence of plasmaspheric hiss. *Journal of Geophysical Research*, *109*, A06209. https://doi.org/10.1029/2004JA010387

Millan, R. M., & Thorne, R. M. (2007). Review of radiation belt relativistic electron losses. *Journal of Atmospheric and Solar: Terrestrial Physics*, *69*, 362–377. https://doi.org/10.1016/j.jastp.2006.06.019

Ni, B., Bortnik, J., Thorne, R. M., Ma, Q., & Chen, L. (2013). Resonant scattering and resultant pitch angle evolution of relativistic electrons by plasmaspheric hiss. *Journal of Geophysical Research: Space Physics*, *118*, 7740–7751. https://doi.org/10.1002/2013JA019260

Ni, B., Cao, X., Zou, Z., Zhou, C., Gu, X., Bortnik, J., … Xie, L. (2015). Resonant scattering of outer zone relativistic electrons by multiband EMIC waves and resultant electron loss time scales. *Journal of Geophysical Research: Space Physics*, *120*, 7357–7373. https://doi.org/10.1002/2015JA021466

Ni, B., Li, W., Thorne, R. M., Bortnik, J., Ma, Q., Chen, L., … Claudepierre, S. G. (2014). Resonant scattering of energetic electrons by unusual low-frequency hiss. *Geophysical Research Letters*, *41*, 1854–1861. https://doi.org/10.1002/2014GL059389

Ni, B., Thorne, R. M., Shprits, Y. Y., & Bortnik, J. (2008). Resonant scattering of plasma sheet electrons by whistler-mode chorus: Contribution to diffuse auroral precipitation. *Geophysical Research Letters*, *35*, L11106. https://doi.org/10.1029/2008GL034032

Roberts, C., & Schulz, M. (1968). Bounce resonant scattering of particles trapped in the Earth's magnetic field. *Journal of Geophysical Research*, *73*(23), 7361–7376. https://doi.org/10.1029/JA073i023p07361

Shprits, Y. Y. (2009). Potential waves for pitch angle scattering of near-equatorially mirroring energetic electrons due to the violation of the second adiabatic invariant. *Geophysical Research Letters*, *36*, L12106. https://doi.org/10.1029/2009GL038322

Shprits, Y. Y. (2016). Estimation of bounce resonant scattering by fast magnetosonic waves. *Geophysical Research Letters*, *43*, 998–1006. https://doi.org/10.1002/2015GL066796

Shprits, Y. Y., & Ni, B. (2009). Dependence of the quasi-linear scattering rates on the wave normal distribution of chorus waves. *Journal of Geophysical Research*, *114*, A11205. https://doi.org/10.1029/2009JA014223

Shprits, Y. Y., Subbotin, D. A., Meredith, N. P., & Elkington, S. R. (2008). Review of modeling of losses and sources of relativistic electrons in the outer radiation belts: II. Local acceleration and loss. *Journal of Atmospheric and Solar: Terrestrial Physics*, *70*(14), 1694–1713. https://doi.org/10.1016/j.jastp.2008.06.014

Spasojevic, M., Shprits, Y. Y., & Orlova, K. (2015). Global empirical models of plasmaspheric hiss using Van Allen Probes. *Journal of Geophysical Research: Space Physics*, *120*, 10,370–10,383. https://doi.org/10.1002/2015JA021803

Summers, D., & Thorne, R. M. (2003). Relativistic electron pitch angle scattering by electromagnetic ion cyclotron waves during geomagnetic storms. *Journal of Geophysical Research*, *108*(A4), 1143. https://doi.org/10.1029/2002JA009489

Summers, D., Ni, B., & Meredith, N. P. (2007a). Timescales for radiation belt electron acceleration and loss due to resonant wave-particle interactions: 2. Evaluation for VLF chorus, ELF hiss, and electromagnetic ion cyclotron waves. *Journal of Geophysical Research*, *112*, A04207. https://doi.org/10.1029/2006JA011993

Summers, D., Ni, B., & Meredith, N. P. (2007b). Timescales for radiation belt electron acceleration and loss due to resonant wave-particle interactions: 1. Theory. *Journal of Geophysical Research*, *112*, A04206. https://doi.org/10.1029/2006JA011801

Summers, D., Ni, B., Meredith, N. P., Horne, R. B., Thorne, R. M., Moldwin, M. B., & Anderson, R. R. (2008). Electron scattering by whistler-mode ELF hiss in plasmaspheric plumes. *Journal of Geophysical Research*, *113*, A04219. https://doi.org/10.1029/2007JA012678

Tao, X., & Li, X. (2016). Theoretical bounce resonance diffusion coefficient for waves generated near the equatorial plane. *Geophysical Research Letters*, *43*, 7389–7397. https://doi.org/10.1002/2016GL070139

Tao, X., Zhang, L., Wang, C., Li, X., Albert, J. M., & Chan, A. A. (2016). An efficient and positivity-preserving layer method for modeling radiation belt diffusion processes. *Journal of Geophysical Research: Space Physics*, *121*, 305–320. https://doi.org/10.1002/2015JA022064

Thorne, R. M. (2010). Radiation belt dynamics: The importance of wave-particle interactions. *Geophysical Research Letters*, *37*, L22107. https://doi.org/10.1029/2010GL044990

Thorne, R. M., Smith, E. J., Burton, R. K., & Holzer, R. E. (1973). Plasmaspheric hiss. *Journal of Geophysical Research*, *78*(10), 1581–1596. https://doi.org/10.1029/JA078i010p01581

Tsurutani, B. T., Falkowski, B. J., Pickett, J. S., Santolik, O., & Lakhina, G. S. (2015). Plasmaspheric hiss properties: Observations from Polar. *Journal of Geophysical Research: Space Physics*, *120*, 414–431. https://doi.org/10.1002/2014JA020518

Usanova, M. E., Drozdov, A., Orlova, K., Mann, I. R., Shprits, Y., Robertson, M. T., … Wygant, J. (2014). Effect of EMIC waves on relativistic and ultrarelativistic electron populations: Ground-based and Van Allen Probes observations. *Geophysical Research Letters*, *41*, 1375–1381. https://doi.org/10.1002/2013GL059024